The Canadian Mineralogist
Vol. 37, pp. 1147-1161 (1999)

PGE DISTRIBUTION IN BASE-METAL ALLOYS AND SULFIDES OF THE NEW CALEDONIA OPHIOLITE

THIERRY AUGÉ[§]

BRGM, B.P. 6009, F-45060 Orléans Cedex 2, France

LOUIS J. CABRI[§]

CANMET, MMSL, 555 Booth Street, Ottawa, Ontario K1A 0G1, Canada

OLIVIER LEGENDRE

BRGM, B.P. 6009, F-45060 Orléans Cedex 2, France

GREG McMAHON

CANMET, MTL, 568 Booth Street, Ottawa, Ontario K1A 0G1, Canada

ALAIN COCHERIE

BRGM, B.P. 6009, F-45060 Orléans Cedex 2, France

Abstract

An Upper Eocene ophiolite nappe covering some 40% of New Caledonia consists of depleted mantle harzburgites, locally covered by mafic and ultramafic cumulates. These mantle harzburgites in places show an enrichment in sulfide and alloy (heazlewoodite, pentlandite, awaruite, millerite and native copper), accompanied by anomalous concentrations of the PGE, as revealed by the whole-rock analyses of three sulfide-enriched samples and by the heavy-mineral concentrates obtained from these samples (up to 1835 ppb Ir, 1527 ppb Rh, 9718 ppb Pt, 11,494 ppb Pd and 988 ppb Au). Although studies to determine the PGE-carrier minerals by SEM were unsuccessful, SIMS depth profiles show that Pt is strongly enriched in awaruite, albeit varying widely among grains, *e.g.*, from 4 to 1210 ppm for 21 grains in one sample. In contrast, 11 grains of pentlandite from the same sample do not exceed 10 ppm Pt, whereas 10 out of 12 grains of heazlewoodite show no detectable Pt, and the Pt content of the other two grains is estimated to be very low (<1 ppm). SIMS ion images thus confirm that awaruite is a preferential host for Pt and that the Pt concentration could be related to the mineral's Fe, Cu, Ni and Co content. These images also show that the awaruite, whether or not Pt-bearing, contains some Au, whereas the heazlewoodite is Au-free. Textural features and trace-element distributions of the ore minerals suggest that the mineralization occurred in a two-step process. In the initial mineralizing event, primary PGE-bearing base-metal sulfides (BMS) crystallized in intergranular positions among the silicates. The second step was related to serpentinization and involved transformation of the primary BMS assemblage to the present secondary assemblage of heazlewoodite, awaruite, and pentlandite, but with a different pattern of PGE distribution.

Keywords: PGE, Au, awaruite, pentlandite, heazlewoodite, secondary-ion mass spectrometry, ophiolite, New Caledonia.

Sommaire

Le complexe ophiolitique de Nouvelle-Calédonie, mis en place à l'Éocène supérieur et qui occupe environ 40% de l'île, est constitué de péridotites mantelliques appauvries, sur lesquelles reposent par endroits des cumulats mafiques et ultramafiques. Localement, les harzburgites mantelliques sont enrichies en sulfures et alliages de métaux de base (heazlewoodite, pentlandite, awaruite, millérite et cuivre natif); certaines montrent des teneurs anomales en EGP. Des concentrés de sulfures et alliages réalisés à partir de ces échantillons ont des teneurs élevées en EGP (maximum 1835 ppb Ir, 1527 ppb Rh, 9718 ppb Pt, 11,494 ppb Pd and 988 ppb Au). Une première étude au MEB n'a pas permis d'identifier de porteurs des EGP. Cependant, une étude à la sonde ionique (SIMS) montre que le Pt se concentre fortement dans l'awaruite, avec des teneurs variant sur 21 grains de 4 à 1210 ppm dans un même échantillon. En revanche, des mesures sur 11 grains de pentlandite du même échantillon montrent des teneurs

§ *E-mail addresses*: t.auge@brgm.fr, lcabri@nrcan.gc.ca

qui n'excèdent pas 10 ppm Pt. Sur 12 grains de heazlewoodite analysés, 10 ont des teneurs en Pt non détectables, et deux donnent des valeurs très faibles (estimées à moins de 1 ppm). Des images de répartition réalisées à la sonde ionique confirment que l'awaruite est le principal porteur de Pt et que la teneur en Pt de l'awaruite pourrait être liée à sa composition (teneurs en Fe, Cu, Ni, Co). Les images SIMS montrent également que l'awaruite, platinifère ou non, contient Au, alors que la heazlewoodite n'en contient pas. La texture des minéraux métalliques et leur composition indiquent que la minéralisation résulte d'un processus à deux étapes. Dans un premier temps (stade magmatique), des sulfures de métaux de base enrichis en EGP vont cristalliser entre les silicates. Dans un second temps, cette paragenèse primaire, sous l'effet de la serpentinisation, va donner un assemblage minéral secondaire composé de heazlewoodite, awaruite, et pentlandite, avec une redistribution des EGP.

Mots-clés: EGP, Au, awaruite, pentlandite, heazlewoodite, spectrométrie de masse des ions secondaires (SIMS), ophiolite, Nouvelle-Calédonie.

Introduction

Mantle peridotites in ophiolite complexes either consist of dunite and harzburgite (depleted "residual" peridotite) or lherzolite (undepleted or "fertile" peridotite), with all intermediate stages between the two. Mantle peridotites can also be depleted rocks impregnated by percolating magma, and therefore show characteristics similar to "fertile" lherzolites. Base-metal sulfides are commonly present in trace amounts in these facies. However, there are places where sulfides are abundant, to the point of forming occurrences mapped by prospectors. Such is the case of the Massif du Sud harzburgite (Fig. 1) in the mantle series of the New Caledonia ophiolite complex (located in the Pacific Ocean, 1500 km east of the Australian Coast), otherwise interpreted as a residual peridotite.

Special attention was paid to these base-metal sulfide (and associated metallic alloy) occurrences during an inventory of the platinum-group element (PGE) resources of New Caledonia. Five sulfide occurrences were sampled and analyzed for the six PGE. Because some of the samples showed an anomalous spectrum relative to sulfide-free mantle peridotites (although with very low values), these were examined in detail. In this article, we present the results of this study, including a description of the occurrences, the mineralogy and composition of the ore minerals, and the chemistry of the mineralized rocks and ore mineral concentrate. We also provide preliminary results of a study of trace Pt in the

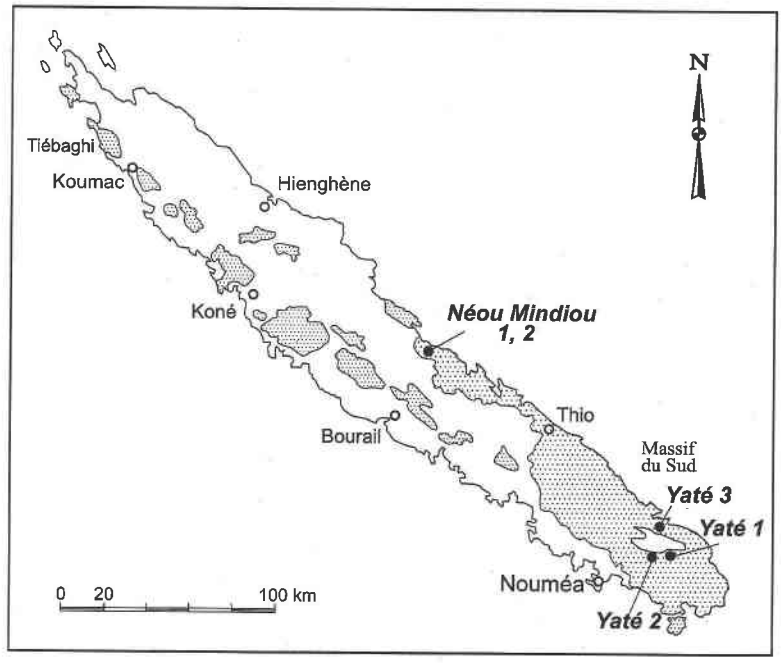

FIG. 1. Simplified geological map of New Caledonia showing the studied sulfide-rich sites in the Massif du Sud. Occurrences Yaté 1, 2 and 3 are located around Lake Yaté.

ore minerals using secondary ion mass spectrometry (SIMS).

Geological Setting

The ultramafic nappe, which covers about 40% of New Caledonia (Fig. 1), represents the lower part of an ophiolite complex emplaced during the Late Eocene (Paris *et al.* 1979). Three units are distinguished: (1) the northern massifs (north of Koumac) consisting of mantle peridotite marked by the presence of plagioclase and spinel lherzolite and an abundance of chromitite occurrences (Moutte 1982, Johan & Augé 1986), (2) the intermediate massifs (on the west Coast) consisting of harzburgite, and (3) the Massif du Sud forming the southern third of the Island. The Massif du Sud is composed of mantle rocks (harzburgite with minor dunite and small bodies of chromitite) upon which cumulate dunite, wehrlite, pyroxenite and gabbro have been recognized locally (Prinzhofer *et al.* 1980). The other parts of the ophiolite sequence are missing.

Sulfide Occurrences

The presence of base-metal sulfides (BMS) in the mantle peridotite of the New Caledonia ophiolite nappe has been recorded since the early 20th century (Glasser 1904). These sulfides were even once considered to be the source of the supergene Ni deposits, which are now known to be derived from the weathering of olivine containing ~0.3 wt% Ni in sulfide-poor ultramafic rocks and not from the sulfide-bearing rocks described below.

Numerous other BMS occurrences in the mantle peridotite have been documented and studied since the first discovery. Picot (1959) carried out the first mineralogical study on three occurrences, describing a sample containing heazlewoodite, partly altered to millerite, and another containing millerite and bravoite (possible alteration of pentlandite). Ramdohr (1967) gave a detailed description of sulfide minerals in peridotite, particularly in samples from New Caledonia. Guillon (1969) showed that the sulfides in the Massif du Sud are concentrated preferentially in the pyroxene-enriched horizons (defining the foliation) of the harzburgite. A detailed study on the distribution of sulfides in the New Caledonia ultramafic massifs (Guillon & Saos 1971) was followed by a description of the main occurrences and their mineralization characteristics (Saos 1972), with further mineralogical descriptions being given by Guillon & Lawrence (1973). At the time, the peridotite was considered to be a cumulate belonging to a "large stratiform massif". The fact that this harzburgite is a residual mantle rock belonging to an ophiolite complex was not recognized until later (Aubouin *et al.* 1977).

All the sulfide occurrences have been found in mantle harzburgite consisting of olivine (70%) with a relatively low degree of serpentinization of the olivine (between 20 and 40%), with orthopyroxene, minor clinopyroxene and chromite constituting the other 30%. There is no difference in terms of mineral composition between the sulfide-bearing and sulfide-free residual mantle peridotites (Johan & Augé 1986). Of note, however, is the association of the ore minerals in two occurrences (Yaté 2 and 3), with spectacular examples of the symplectitic texture (Fig. 2) that is common in mantle peridotite (Field & Haggerty 1994), particularly in the peridotites of New Caledonia.

Five sulfide occurrences were studied in the Massif du Sud, three in the south (Yaté 1, 2, 3) and two in the north (Néou Mindiou 1, 2).

Yaté 1 occurrence

This is the largest of the five occurrences studied. In the field, sulfides were identified in large, quasi *in situ* boulders of peridotite (up to 1 m in diameter) extending over an area of about 1000 m^2 in a zone of thin lateritic overburden. In a given boulder, the sulfides occur in small, highly discontinuous layers, from 20 to 30 cm in length and up to 1 cm in thickness. The sulfide content is low, estimated at 10% maximum in a hand specimen, with some grains up to 5 mm in size.

The ore mineral assemblage consists of heazlewoodite, pentlandite and awaruite. In addition, rods of millerite are found in heazlewoodite, and native copper occurs on the periphery of heazlewoodite and awaruite grains. Heazlewoodite, the most abundant mineral, occurs either in isolated grains or in association with awaruite and pentlandite. Pentlandite rarely occurs as isolated grains, and is most commonly present as a halo around heazlewoodite, which suggests a late crystallization. Awaruite occurs as isolated grains, in association with heazlewoodite or as rods or irregular grains included within the heazlewoodite. Graphite also is found, generally in association with chromite grains and heazlewoodite.

The associations and textures of the ore minerals are unusual. The ore minerals are commonly associated with chromite (Fig. 2A) and form in an arc around silicates, as illustrated in Figure 2B and 2C, where locally chromite forms a link between the sulfides (Fig. 2D). The texture exhibited by the BMS resembles that of the chromite grains, *i.e.*, occurring interstitially between and molded to silicates. Aside from these large grains of BMS, small inclusions of BMS are found in the silicates, particularly in orthopyroxene (similar to Fig. 2E).

Yaté 2 and 3 occurrences

The ore minerals are found in small boulders, which occur free and virtually *in situ*, over an area of about 250 m^2. The boulders had to be broken in order to see the ore minerals, as they are not visible on the weathered surface. The Yaté 2 occurrence is characterized by symplectitic intergrowths of chromite and silicates (mainly orthopyroxene, generally altered) with associ-

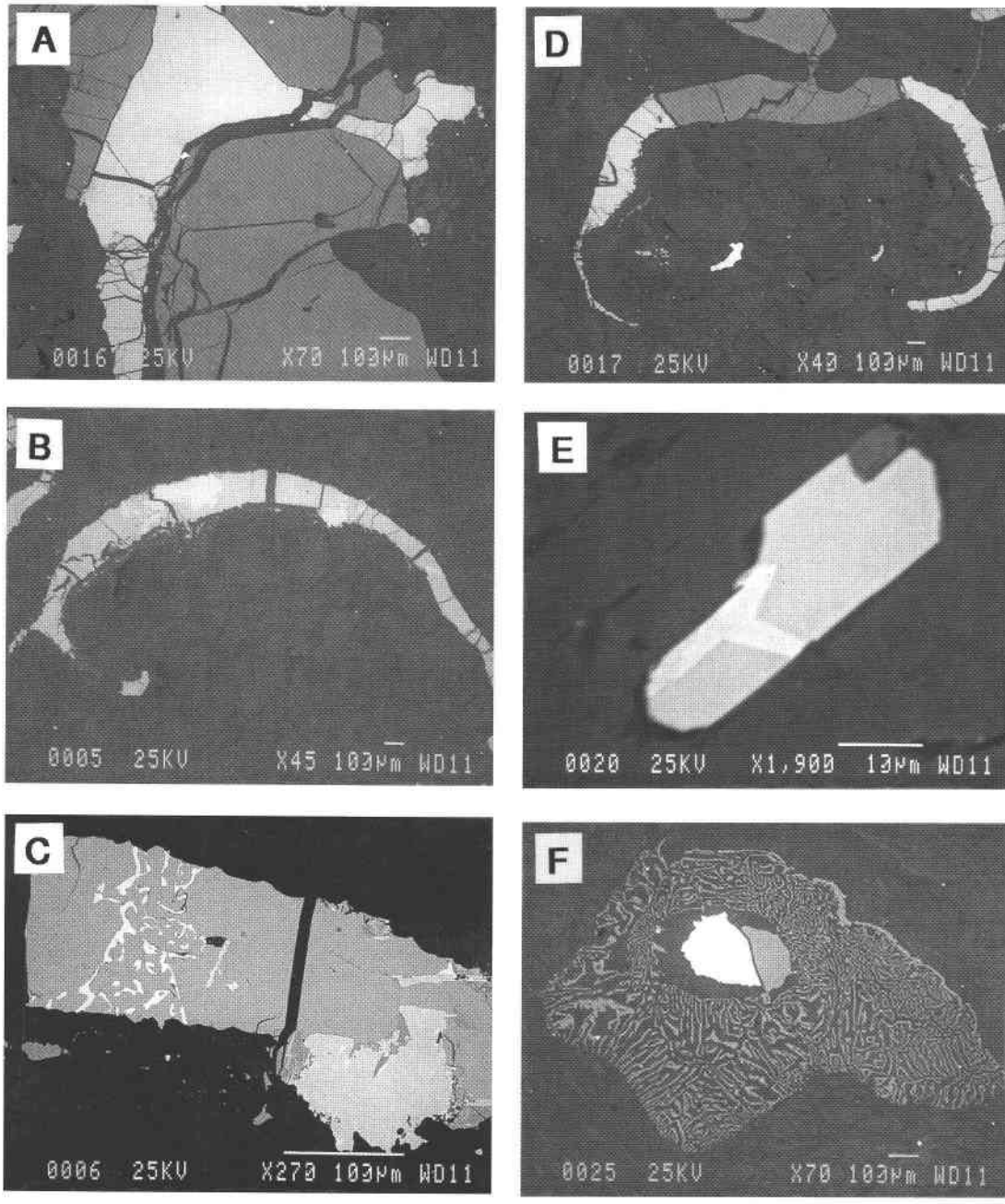

FIG. 2. SEM images in the back-scattered electron (BSE) mode. Scale bar is given on each image. A. Typical chromite (dark grey) – base metal sulfide (BMS) association (heazlewoodite: white, pentlandite: pale grey). Sample 165–1D, Yaté 1 occurrence. B. Typical texture of BMS (heazlewoodite, pentlandite) and awaruite forming an arc of a circle in an olivine and serpentine matrix. Sample 165–1A, Yaté 1 occurrence. C. Detail of B showing awaruite (light grey) and heazlewoodite (dark grey) with exsolution of native Cu (white). D. Image showing the relationships between BMS (heazlewoodite and pentlandite, white), chromite (light grey) and silicate matrix (olivine and serpentine, dark grey). Sample 165–1D, Yaté 1 occurrence. E. Euhedral composite inclusion (pentlandite: dark grey, heazlewoodite: light grey) in a pyroxene crystal. Sample 188A, Néou Mindiou 1 occurrence. F. Type-1 symplectite; chromite – orthopyroxene association with a core containing crystals of awaruite (white) and chromite (grey). Sample 165–2B, Yaté 2 occurrence.

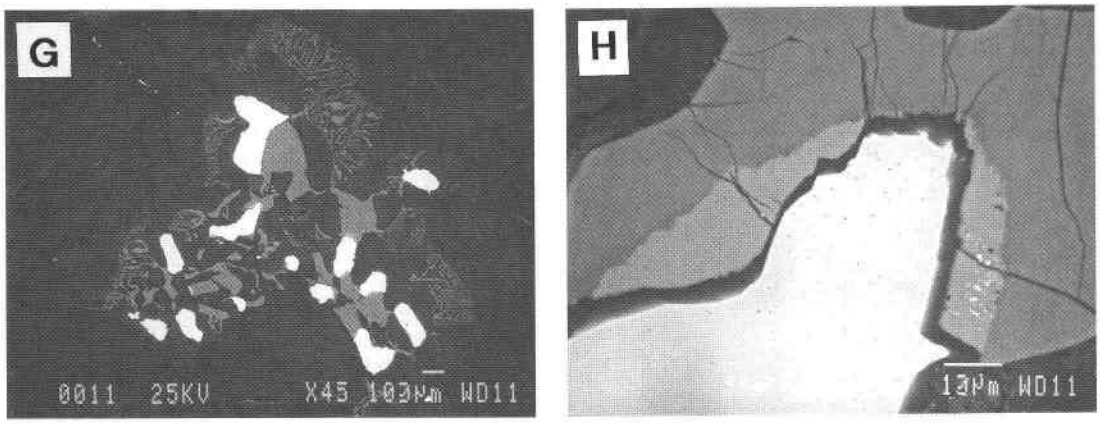

FIG. 2. (continued). G. Complex association of a chromite – orthopyroxenite symplectite containing crystals of chromite (dark grey) and awaruite (white). Sample 165–3A, Yaté 3 occurrence. H. Reaction rim in chromite (dark grey) at its contact with awaruite (white). Sample 165–3A, Yaté 3 occurrence.

ated awaruite. Where awaruite is present, it is located at the center of the symplectite; the example depicted in Figure 2F shows an adjacent chromite crystal. The vermicular intergrowths of chromite are very fine (type-1 symplectite). The same samples also show finer domains of symplectite without awaruite; these are intergrowths of chromite and of orthopyroxene and olivine. No BMS was found in either of the two samples studied.

The Yaté 3 occurrence also is characterized by chromite – silicate – awaruite symplectites of which two types are present. The first is analogous to that described from Yaté 2 (type 1, Fig. 2F), and the second (type 2) consists of an assemblage of chromite + awaruite in silicates (Fig. 2G), with the chromite and awaruite forming more compact grains than in the symplectites of the first type. An unusual phase, tentatively interpreted as a reaction rim, may be seen between chromite and awaruite (Fig. 2H). Heazlewoodite also is present, in some cases in abundance, with a halo of pentlandite and a rim of awaruite and native copper.

Néou Mindiou occurrences

These two occurrences are about 700 m apart. At Néou Mindiou 1 (NM1), a 1- to 2-cm-thick layer of discontinuous sulfides is visible in several boulders, and the sulfide horizon is conformable to the foliation defined by the orthopyroxene horizons. In the Néou Mindiou 2 (NM2) occurrence, boulders enriched in ore minerals were found on a steep slope. The structural arrangement of the mineralization could not be observed.

The mineralization at Néou Mindiou 1 includes large grains of pentlandite (which is abundant and very prominent here) in an orthopyroxene-rich horizon with veinlets of heazlewoodite. Exsolution domains of cubanite and millerite in heazlewoodite occur locally, with a surface alteration to covellite and native copper. Abundant smaller grains of BMS are included in the pyroxene (Fig. 2E).

The mineralization at Néou Mindiou 2 includes rare disseminated pentlandite, invariably surrounded by an aureole of awaruite. Chromite locally moulds pentlandite grains, and the rock is quite heavily serpentinized.

PGE ABUNDANCES

Analysis of a sulfide-bearing rock sample from each of the five occurrences was done by inductively coupled plasma – mass spectrometry (ICP–MS) after nickel sulfide fusion in routine conditions by XRAL Laboratories (Ancaster, Ontario, Canada). The results, normalized to a sulfide-free peridotite of New Caledonia, show three types of profile (Fig. 3, Table 1): (i) a spectrum with a positive slope and enrichment in Pt, Pd and Au (concentrations up to 110, 41 and 14 ppb, respectively) for the two Néou Mindiou occurrences, (ii) a V-shape profile marked by Pt depletion for the Yaté 1 sample, but with values quite close to those of sulfide-free harzburgite for the other PGE, and (iii) a sawtooth spectrum with very low values (lower than the reference harzburgite) for the Yaté 2 and 3 occurrences. It may be noted that the Pt:Pd ratio is low (between 0.23 and 0.40) for the three Yaté occurrences, whereas it increases to 0.67 for the Néou Mindiou 1 occurrence and to 2.68 for the Néou Mindiou 2 occurrence.

PGE GEOCHEMISTRY OF THE MINERALS

Following the ICP–MS results obtained on the rock samples, we carried out a systematic search for PGM in these samples. As a search for PGM by ore microscopy and scanning electron microscopy (SEM) was unsuccessful, it was decided to concentrate the ore minerals

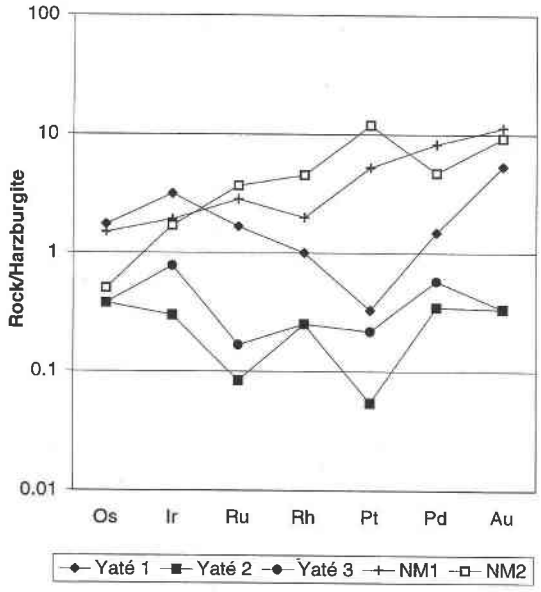

FIG. 3. PGE content of the different sulfide-bearing peridotites normalized to mantle harzburgite from New Caledonia. Normalization values (in ppb): Os 4, Ir 2.7, Ru 6, Rh 2, Pt 9.2, Pd 8.7, Au 1.5 (Augé *et al.*, 1995) (NM1, 2: Néou Mindiou 1 and 2 occurrences). For PGE values below the detection limit (DL), half of the DL was used.

and to work on the concentrates. The samples were crushed, ground, and sieved for mineral separation; "mini-panner" and heavy-liquid separations were made to produce concentrates of the ore minerals that were mounted as polished sections for microscopic examination and later remounted in graphite-loaded polished sections for micro-analytical procedures. Examination of the concentrates by scanning electron microscopy (SEM) revealed only two PGM, less than five μm in size. The first is a Pt–Fe alloy (determined qualitatively) adjacent to a crystal of awaruite (sample 165–2, Yaté 1), and the second is a Pd–Cu alloy, attached to an altered rim of pentlandite (sample 188, Néou Mindiou 1). Our preliminary conclusion was that the PGE could be in solid solution in the BMS.

A portion of the ore-mineral concentrates was then prepared for chemical analyses, using neutron activation (Cocherie *et al.* 1987) for Ir, Pt, Pd and Au, and alpha-particle activation for Rh (Volfinger 1989). The concentrations of the other elements shown in Table 1 were also established by neutron activation; the levels of Cu, Os and Ru were not determined. In two occurrences (Yaté 2 and Néou Mindiou 1), the chromite separates were also analyzed for Ir, Pt, Pd and Au.

In terms of composition, the ore minerals from the Yaté occurrences are clearly distinct from those of the Néou Mindiou occurrences. The former are characterized by a low Fe/Ni value, between 0.10 and 0.14, compared to 0.58 and 0.73 for the latter, whereas the latter have high Co concentrations, between 2200 and 2400 ppm, in comparison with 820 to 1450 for former. These differences correspond to the difference in the nature of

TABLE 1. GEOCHEMICAL DATA FOR SEPARATED ORE MINERALS AND WHOLE ROCK (SULFIDE-BEARING), NEW CALEDONIA OPHIOLITE

		Os ppb	Ir ppb	Ru ppb	Rh ppb	Pt ppb	Pd ppb	Au ppb	Fe %	Ni %	Cr_2O_3 %	Co ppm	Zn ppm	As ppm	Sb ppm	$\delta^{34}S$ ‰
Base metal and alloy separates																
Yaté 1	165-1S	-	1835	-	795	9657	4773	988	6.60	60.28	0.58	1304	93	-31	0.84	-1.9
Yaté 2	165-2S	-	1745	-	1527	9718	3761	777	6.30	60.47	0.43	1448	26	32	0.62	-2.0
Yaté 3	165-3S	-	568	-		1570	2522	297	8.40	60.25		824	531	191	2.19	-0.1
Néou Mindiou1	188S	-	402	-	1176	1954	11494	286	17.80	30.71	1.60	2374	107	463	9.61	-0.2
Néou Mindiou 2	190S	-	924	-		6875	7124	341	21.00	28.86	0.92	2261	77	-19	0.12	-2.3
Chromite separates																
Yaté 2	165-2Cr	-	21	-	-	623	137	15								
Néou Mindiou1	188Cr	-	107	-	-	390	1002	35								
Whole rock																
Yaté 1	165-1	7	8.5	10	2	3	13	8								
Yaté 2	165-2	<3	0.8	<1	<1	<1	3	<1								
Yaté 3	165-3	<3	2.1	1	<1	2	5	<1								
Néou Mindiou1	188	6	5.2	17	4	48	72	17								
Néou Mindiou 2	190	<4	4.6	22	9	110	41	14								
Apparent partition coefficient of base metal sulfide-alloy/whole rock																
Yaté 1	165-1S		417		398	1050	1085	706								
Yaté 2	165-2S		397		764	1056	855	555								
Yaté 3	165-3S		113			149	501	185								
Néou Mindiou1	188S		91		588	212	2612	204								
Néou Mindiou 2	190S		210			747	1619	244								

the sulfides, with heazlewoodite (Ni_3S_2) predominating in the Yaté material and pentlandite [$(Fe,Ni,Co)_9S_8$] predominating in the Néou Mindiou material. It should be noted that the Cr content of the heavy-mineral concentrates remains low, between 0.43 and 1.60% Cr_2O_3, which means that the analyzed samples contain very little chromite.

High values for precious metals were determined in the heavy-mineral concentrates, with maximum values of 1835 ppb Ir, 1527 ppb Rh, 9718 ppb Pt, 11,494 ppb Pd and 988 ppb Au, depending on the sample (Table 1). The Pt:Pd ratio is discriminant (Fig. 4A), with three distributions being found: (i) Pt/Pd close to 2, with high Pt concentrations (Yaté 1 and Yaté 2), (ii) a ratio close to 1, with high concentrations (Néou Mindiou 2) or low concentrations (Yaté 3), and (iii) a ratio much less than 1, with very high Pd concentrations (Néou Mindiou 1). For all three types of distribution with high concentrations, the Pt + Pd content is surprisingly constant, between 13,448 and 14,430 ppb, with good negative correlation. The sample from Yaté 3, with a Pt:Pd ratio of 0.62, has a much lower concentration (Pt + Pd = 4092 ppb). The samples with pentlandite predominating (Néou Mindiou 1 and 2) thus appear to have the highest Pd content.

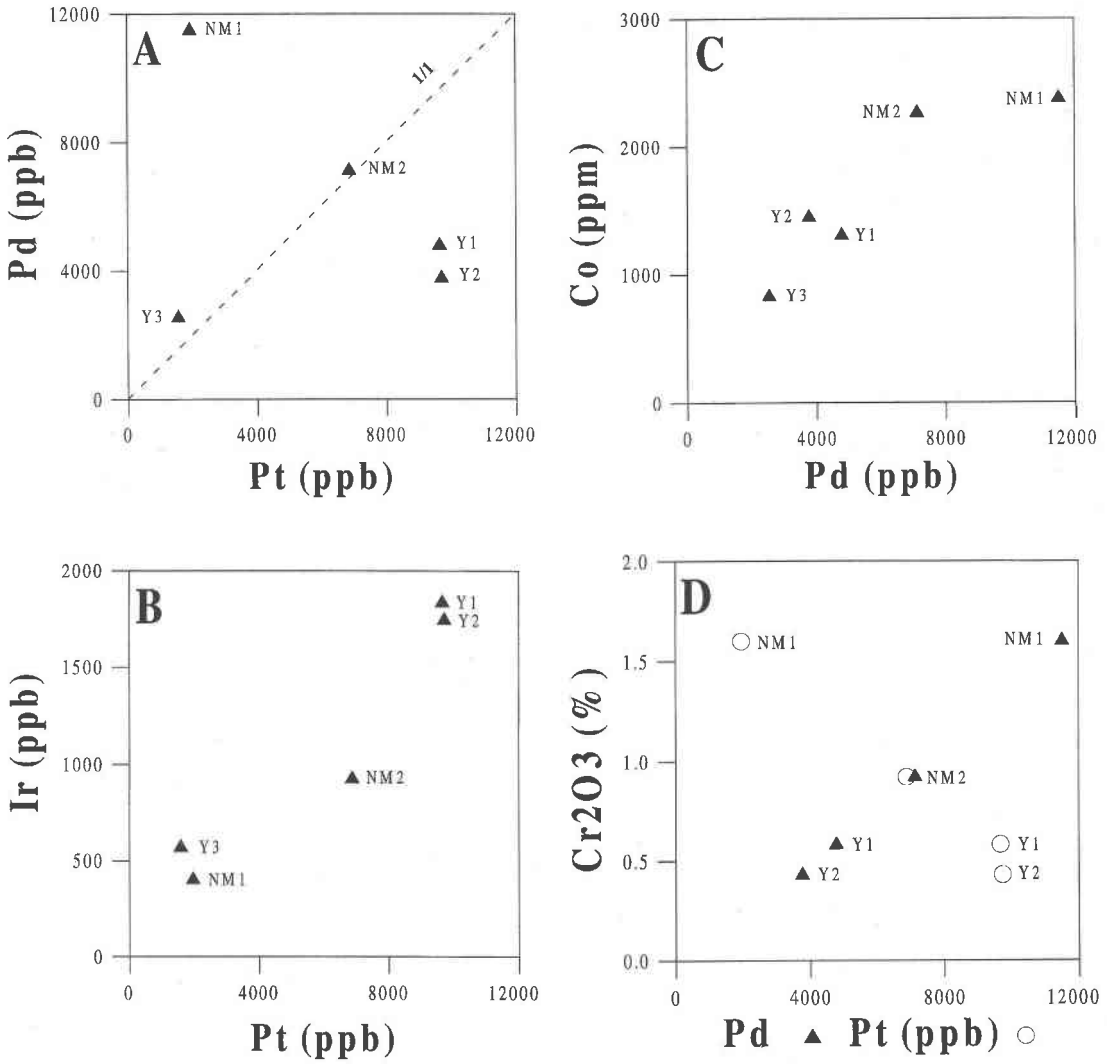

FIG. 4. Correlation diagrams for ore-mineral separates from the different sulfide-bearing peridotites. A: Pd–Pt, B: Ir–Pt, C: Co–Pd, D: Cr_2O_3–Pd and Pt. Y1, 2, 3: Yaté 1, 2 and 3 occurrences; NM1, 2: Néou Mindiou 1 and 2 occurrences.

TABLE 2. COMPOSITION OF HEAZLEWOODITE AND PENTLANDITE, NEW CALEDONIA OPHIOLITE

Occurrence	Y1	Y1	Y1	Y1	Y3	Y3	Y3	NM1	NM1	Y1	Y1	Y1	Y1	Y3	Y3	Y3	NM1	NM1	NM1
Analysis no	11	28	40	HZ1*	50	51	64	61	62	25	29	75	PN1**	56	67	69	60	87	88
Heazlewoodite										**Pentlandite**									
Weight percent																			
Ni	73.12	72.86	73.37	73.46	72.29	72.24	72.88	73.07	73.47	29.12	34.01	33.33	34.61	30.82	32.03	33.58	33.47	34.34	34.46
S	26.89	27.03	27.03	26.68	27.09	26.81	27.43	26.75	26.70	32.87	33.18	33.48	33.13	33.50	33.46	33.10	33.38	33.34	33.42
Fe	0.17	0.06	0.00	0.38	0.39	0.25	0.07	0.24	0.19	24.31	30.66	31.76	31.45	33.81	32.76	31.94	31.91	31.07	31.15
As	0.00	0.00	0.00	0.03	0.16	0.16	0.01	0.03	0.00	0.02	0.03	0.03	0.03	0.04	0.06	0.00	0.09	0.04	0.02
Cu	0.02	0.00	0.02	0.02	0.03	0.02	0.06	0.01	0.00	0.14	0.00	0.09	0.05	0.05	0.02	0.05	0.00	0.23	0.07
Pb	0.01	0.00	0.00	nd	0.06	0.06	0.02	0.02	0.04	0.08	0.12	0.12	nd	0.11	0.12	0.06	0.13	0.07	0.00
Co	0.11	0.00	0.01	0.00	0.07	0.05	0.00	0.00	0.00	13.06	1.32	1.40	0.75	1.34	0.89	0.48	0.59	0.38	0.35
Cr	0.00	0.00	0.00	nd	0.40	0.35	0.00	0.00	0.00	0.00	0.00	0.09	nd	0.01	0.00	0.02	0.00	0.00	0.00
Total	100.32	99.96	100.42	100.58	100.49	99.94	100.47	100.12	100.41	99.59	99.32	100.30	100.03	99.68	99.33	99.21	99.58	99.47	99.48
Atomic percent																			
Ni	0.596	0.595	0.597	0.598	0.588	0.591	0.591	0.597	0.599	0.227	0.265	0.257	0.268	0.239	0.249	0.262	0.260	0.267	0.267
S	0.401	0.404	0.403	0.398	0.403	0.402	0.408	0.400	0.399	0.470	0.473	0.473	0.470	0.475	0.476	0.472	0.474	0.474	0.475
Fe	0.001	0.001	0.000	0.003	0.003	0.002	0.001	0.002	0.002	0.200	0.251	0.257	0.256	0.275	0.268	0.262	0.260	0.254	0.254
As	0.000	0.000	0.000	0.000	0.001	0.001	0.000	0.000	0.000	0.000	0.000	0.000	0.000	0.000	0.000	0.000	0.001	0.000	0.000
Cu	0.000	0.000	0.000	0.000	0.000	0.000	0.000	0.000	0.000	0.001	0.000	0.001	0.000	0.000	0.000	0.000	0.000	0.002	0.001
Pb	0.000	0.000	0.000	-	0.000	0.000	0.000	0.000	0.000	0.000	0.000	0.000	-	0.000	0.000	0.000	0.000	0.000	0.000
Co	0.001	0.000	0.000	0.000	0.001	0.000	0.000	0.000	0.000	0.102	0.010	0.011	0.006	0.010	0.007	0.004	0.005	0.003	0.003
Cr	0.000	0.000	0.000	-	0.004	0.003	0.000	0.000	0.000	0.000	0.000	0.001	-	0.000	0.000	0.000	0.000	0.000	0.000

Results of electron-probe micro-analyses. * Composition of heazlewoodite shown in Figure 6. ** Composition of pentlandite shown on Figure 6.

Figure 4B shows a positive correlation between Ir and Pt. The Ir concentrations vary between 402 and 1835 ppb, indicating a clear affinity between Pt and Ir in this type of environment. The level of Rh was determined in only three samples, with values between 795 and 1527 ppb that seem to be independent of the Pt/Pd value.

The Au concentrations are about 1 ppm in Yaté 1 and between 286 and 777 ppb in the other samples, without any significant variations.

Two interesting correlations are found. The first is Co–Pd (Fig. 4C), which indicates that Pd is essentially associated with pentlandite. The second is more enigmatic, and concerns the Cr content relative to Pt and Pd (Fig. 4D). Cr correlates positively with Pd and negatively with Pt. These latter correlations remain unclear. They cannot be attributed to chromite contamination.

Table 1 shows the average apparent partition coefficients obtained (concentration of the element in the ore mineral divided by concentration of the element in the rock), which are highly variable and probably reflect differences in the composition of the sulfides. The highest Pd values, for example, were obtained for samples rich in pentlandite.

S Isotopes

The S isotope ratios were measured on concentrates of base-metal sulfides and alloys at BRGM by the combustion method. The gases obtained were analyzed for their isotopic composition using a Delta S Finnigan–Mat gas-source mass spectrometer. The results are reported in δ units relative to the CDT standard. Reproducibility was ±0.3‰. The values obtained are consistent and slightly negative, lying between –0.1 and –2.3 (Table 1), compatible with a magmatic origin or derivation from a fluid of magmatic origin.

Composition of the Ore Minerals

The sulfides and awaruite were determined by electron-probe micro-analysis (EPMA) either in polished sections of rock slices or in concentrates mounted in polished sections. EPMA determinations for major and minor elements were done at BRGM (Orléans) using a Cameca SX–50 electron-probe micro-analyzer equipped with wavelength-dispersion spectrometers and operated at the following conditions: acceleration voltage 20 kV, and beam current *ca.* 20 nA.

Heazlewoodite

Heazlewoodite was analyzed from the Yaté 1, Yaté 3 and Néou Mindiou 1 occurrences (Table 2). Regardless of the source, heazlewoodite has a homogeneous composition, close to the ideal stoichiometry Ni_3S_2. Trace Fe was found (up to 0.38 wt%) and, in a few grains, trace concentrations of Cr were measured, but these enrichments are not particularly significant. The other elements are not present in any significant amount.

Pentlandite

Pentlandite was analyzed in samples from Yaté 1, Yaté 3 and Néou Mindiou 1 and found to have a Ni:Fe ratio averaging 1, but ranging between 0.86 and 1.19 in one sample (Table 2). Similarly, very heterogeneous Co values were found in one sample, where a Co-rich pentlandite grain (with 13 wt% Co) was found included in heazlewoodite. In contrast to this extreme value, the following ranges in Co content were found: (a) Yaté 1 from 0.5 to 2.3 wt% (average 1.34 wt%, σ 0.56); (b) Yaté 3 from 0.4 to 1.3 wt% (average 1.02 wt%, σ 0.39), and (c) Néou Mindiou 1 from 0.4 to 0.6 wt% (average 0.45 wt%, σ 0.08).

TABLE 3. COMPOSITION OF AWARUITE, NEW CALEDONIA OPHIOLITE

Occurrence	Y1	Y1	Y1	Y1	Y1	Y1	Y1	Y1	Y1	Y2	Y2	Y2	Y2	Y3	Y3	Y3	Y3	Y3
Analysis no	1	7	16	18	19	20	97	AW1*	AW2**	81 c1	84 r1	85 c2	86 r2	42	47	65	66	93
Awaruite																		
Weight percent																		
Ni	77,49	77,63	79,47	82,15	85,13	81,19	76,58	78,98	77,80	80,85	94,51	80,61	91,62	96,61	99,46	74,48	74,05	98,80
S	0,00	0,00	0,01	0,02	0,01	0,02	0,06	0,01	0,04	0,00	0,02	0,04	0,02	0,02	0,00	0,11	0,10	0,00
Fe	19,83	19,71	17,71	5,03	11,45	15,67	19,99	18,54	19,69	17,57	4,78	17,52	7,79	1,65	0,81	23,72	23,75	1,87
As	0,04	0,01	0,03	0,01	0,04	0,04	0,05	0,04	0,05	0,00	0,06	0,01	0,00	0,00	0,00	0,08	0,01	0,00
Cu	1,55	1,71	1,80	13,30	3,02	2,09	2,27	1,17	2,20	0,07	0,16	0,06	0,03	1,47	0,42	0,17	0,45	0,22
Pb	0,00	0,00	0,06	0,00	0,00	0,00	0,09	nd	nd	0,00	0,05	0,13	0,09	0,00	0,13	0,01	0,07	0,07
Co	0,38	0,38	0,41	0,34	0,28	0,31	0,29	0,34	0,21	0,75	0,29	0,72	0,42	0,05	0,00	0,06	0,09	0,09
Cr	0,00	0,00	0,00	0,00	0,00	0,00	0,00	nd	nd	0,01	0,69	0,00	0,33	0,11	0,00	0,00	0,00	0,02
Total	99,29	99,44	99,49	100,85	99,94	99,32	99,33	99,08	99,98	99,24	100,55	99,09	100,29	99,91	100,82	98,62	98,52	101,07
Atomic percent																		
Ni	0,774	0,774	0,793	0,821	0,849	0,812	0,765	0,790	0,772	0,807	0,937	0,807	0,910	0,967	0,987	0,746	0,742	0,977
S	0,000	0,000	0,000	0,000	0,000	0,000	0,001	0,000	0,001	0,000	0,000	0,001	0,000	0,000	0,000	0,002	0,002	0,000
Fe	0,208	0,207	0,186	0,053	0,120	0,165	0,210	0,195	0,205	0,184	0,050	0,184	0,081	0,017	0,008	0,250	0,250	0,019
As	0,000	0,000	0,000	0,000	0,000	0,000	0,000	0,000	0,000	0,000	0,000	0,000	0,000	0,000	0,000	0,001	0,000	0,000
Cu	0,014	0,016	0,017	0,123	0,028	0,019	0,021	0,011	0,021	0,001	0,001	0,001	0,000	0,014	0,004	0,002	0,004	0,002
Pb	0,000	0,000	0,000	0,000	0,000	0,000	0,000	-	-	0,000	0,000	0,000	0,000	0,000	0,000	0,000	0,000	0,000
Co	0,004	0,004	0,004	0,003	0,003	0,003	0,003	0,003	0,002	0,007	0,003	0,007	0,004	0,000	0,000	0,001	0,001	0,001
Cr	0,000	0,000	0,000	0,000	0,000	0,000	0,000	-	-	0,000	0,008	0,000	0,004	0,001	0,000	0,000	0,000	0,000

Results of electron-probe micro-analyses. * Composition of grain 1, Figure 6. ** Composition of grain 2, Figure 6; r: rim, c: core.

Awaruite

Awaruite was analyzed from the three Yaté occurrences (Table 3). It is found as isolated crystals or associated in a symplectitic intergrowth with chromite, where it occurs either as an isolated crystal in the core of the symplectite (type 1, Fig. 2F), or as small crystals in the symplectite (type 2, Fig. 2G). Awaruite varies greatly in composition from one crystal to another and within a given crystal. The composition is essentially dominated by Ni-for-Fe substitution (Fig. 5); it ranges from close to metallic Ni (Ni 98.7% at.) to a more iron-rich composition (Ni 74.2%, Fe 20.5% at., a composition close to Ni_3Fe, or stoichiometric awaruite). Trace Co and Cu also are found. At Yaté 1, the awaruite systematically yields higher Cu concentrations, up to 13.30 wt% Cu (av. 1.83 wt%, σ 0.39). The Yaté 2 awaruite has the lowest Cu concentrations (av. 0.08 wt%, σ 0.04), whereas it has higher Co concentrations (0.58 wt%, σ 0.18, compared to 0.38 wt%, σ 0.09 for Yaté 1). The Yaté 3 awaruite gives variable Cu values (between 1.47 and 0.17 wt%), but with very low Co concentrations (0.09 wt%, σ 0.07). There is no correlation between variations in the major and minor elements. Moreover, it was found that the Ir content of these samples of awaruite is below the calculated detection threshold for EPMA (around 1000 ppm), in contrast to iridian awaruite and a Ru–Os–Ir–Ni–Fe alloy that were described from an ophiolite from Pakistan (Ahmed & Bevan 1981). Furthermore, no relationship was observed between the habit of the grains (*i.e.*, isolated or in symplectites) and their composition. However, significant zoning occurs; Ni is enriched from the grain center to the perimeter, but was examined only in certain grains (Fig. 5).

An interesting phenomenon was observed in certain type-2 symplectites (and is therefore not systematic). At the contact between awaruite and chromite, an apparent reaction-rim up to 10 μm in width has developed in the chromite, characterized under the ore microscope by a reflectance intermediate between chromite and awaruite. This phase resulted from transformation of the chromite, and occurred prior to its fracturing (Fig. 2H). EPMA analysis of this component shows that it is an oxide of Fe and Ni. The analyses give an average of 23.5 wt% NiO, 22.3% FeO, 51.8% Fe_2O_3 and traces of Si and Mg, with only 0.89 wt% Cr_2O_3 (Table 4), as opposed to between 54 and 58 wt% Cr_2O_3 for the host chromite. The compositions obtained suggest a spinel of the $(Ni,Fe^{2+})Fe^{3+}{}_2O_4$ trevorite type, but the structural formulas

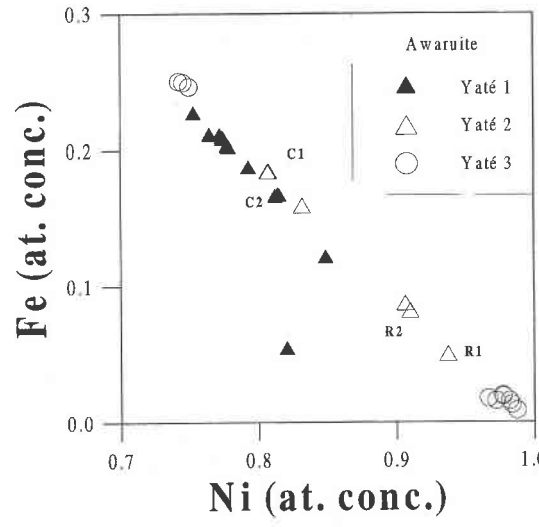

FIG. 5. Fe–Ni (atomic concentration, *i.e.*, atoms per formula unit) correlation diagram for awaruite from the different sulfide-bearing peridotites. C, Core, R, Rim for zoned crystals (analytical results given in Table 3).

TABLE 4. COMPOSITION OF SECONDARY Fe–Ni OXIDE AND CHROMITE, NEW CALEDONIA OPHIOLITE

Occurrence	Y3	Y3	Y3	Y3	Y3	Y3	Y3
Analysis no	34	35	36	37	38	30	39
Fe-Ni oxide						**Chromite**	
Weight percent							
NiO	23.23	24.90	20.60	22.78	23.26	0.47	0.57
SiO_2	0.59	0.35	0.57	0.00	0.03	0.12	0.01
FeO tot	66.48	68.58	73.85	67.40	66.57		
FeO	21.66	22.53	24.26	22.62	22.30	22.71	25.03
Fe_2O_3	50.80	51.17	55.12	52.77	52.20	0.00	0.00
CoO	0.21	0.02	0.30	0.03	0.00	0.45	0.77
Al_2O_3	0.09	0.00	0.01	0.08	0.05	12.72	13.20
MnO	0.10	0.13	0.00	0.04	0.00	0.22	0.17
CaO	0.07	0.01	0.00	0.00	0.04	0.02	0.00
MgO	0.63	0.42	0.56	0.14	0.18	6.81	5.17
V_2O_3	0.09	0.00	0.22	0.00	0.19	1.28	1.21
TiO_2	0.00	0.00	0.00	0.03	0.00	0.00	0.04
Cr_2O_3	0.88	0.82	0.94	0.90	0.95	58.12	54.11
Total	98.40	100.36	102.62	99.41	99.26	102.93	100.28
Atomic percent							
Ni	6.173	6.469	5.156	6.175	6.311	0.098	0.122
Si	0.195	0.113	0.177	0.000	0.012	0.030	0.003
Fe^{2+}	5.986	6.088	6.314	6.377	6.292	4.907	5.607
Fe^{3+}	12.382	12.436	12.909	12.620	12.491	0.000	0.000
Co	0.057	0.004	0.074	0.009	0.001	0.093	0.164
Al	0.036	0.001	0.004	0.030	0.019	3.872	4.168
Mn	0.027	0.036	0.000	0.012	0.000	0.049	0.039
Ca	0.024	0.004	0.000	0.000	0.015	0.005	0.000
Mg	0.312	0.201	0.258	0.070	0.089	2.622	2.064
V	0.020	0.000	0.046	0.000	0.043	0.219	0.214
Ti	0.000	0.000	0.000	0.007	0.000	0.000	0.008
Cr	0.231	0.210	0.231	0.240	0.253	11.871	11.461
Total	25.459	25.562	25.182	25.551	25.557	23.769	23.852

Results of electron-probe micro-analyses. The proportion of Fe^{3+} is calculated on the basis of charge-balance considerations in the spinel structure.

calculated on the basis of 32 atoms of oxygen and equilibration of charges are far from the theoretical formula. On the basis of average values, the formula may be written as $(Ni_{6.3}Fe_{6.2}Mg_{0.2})^{2+}\Sigma_{12.7}(Fe_{12.5}Cr_{0.2}Si_{0.1})^{3+}\Sigma_{12.8}O_{32}$, thus showing a marked deficiency in trivalent elements relative to spinel. Calculation of the structural formula based on the $NiFe_2O_4$ type does not give any better results. This phenomenon (observed systematically where awaruite and chromite are in contact) is paradoxical because, where chromite is in contact with the Ni–Fe alloy, it loses all its chromium (through replacement by Fe^{3+}) and all its Mg (which is replaced by Ni), whereas its FeO content remains constant. The phenomenon occurs abruptly because no chemical zoning is seen in the chromite composition, unlike the awaruite. The latter is enriched in Ni around its edges, which negates *a priori* diffusion of Ni from the awaruite to the chromite. The suggested mechanism is as follows: Ni and Fe diffuse from the awaruite to the chromite and oxidize, and they replace Cr and Mg in the chromite. This process must occur relatively early in the history of the rock, as it is independent of the fracturing of the chromite.

TABLE 5. SIMS ANALYTICAL CONDITIONS (CANMET)

Primary ion beam and polarity	Cs^+
Secondary ion polarity	Negative
Matrix masses measured	^{56}Fe, $^{57}Fe_2+^{32}S$, $^{62}Ni_2+^{32}S$, ^{62}Ni
Primary beam current	350-500 nA
Primary beam accelerating voltage	10 kV
Impact energy	14.5 kV
Field aperture diameter	750 µm
Contrast diaphragm diameter	400 µm
Raster	250 µm
Image field	150 µm
Diameter of analysis area	62.5 µm
Implant standard	Pentlandite
Implantation fluence, species	$1.0x10^{13}$ ions, $^{198}Pt/cm^2$
Counting time per mass per cycle	1 s
Mass resolution	~ 2,000 m/Δm
Energy offset	none
Minimum detection limits Pt: pentlandite	230 - 305 ppbw
Depth of analyzed profiles	0.3 - 2.0 µm

EPMA AND SIMS ANALYSES FOR THE TRACE ELEMENTS

Because of the almost total absence of PGE carriers associated with the ore minerals, it was decided to determine whether trace amounts of PGE occur in solid solution in the ore minerals. We limited this work to Pt, using both EPMA and SIMS (secondary ion mass spectrometry) and, for this preliminary investigation, studied only one sample, from Yaté 1 (sample 165–1). The EPMA analyses for major and minor elements, as well as for trace Pt, were carried out at BRGM (Orléans) using a Cameca SX–50 electron-probe micro-analyzer equipped with wavelength-dispersion spectrometers. For awaruite, the analytical conditions were: acceleration voltage 20 kV, beam current 200 nA, with counting times of 600 s for Pt (peak + background) and 10 s for all the other elements. Under such conditions, the calculated limit of detection for Pt is 100 ppm (2σ confidence level). The following standards were used: pyrite for S, arsenopyrite for As, and pure metals for all the other elements, using the following X-ray lines Pt$L\alpha$, Fe$K\alpha$, Ni$K\alpha$, Cu$K\alpha$, Co$K\alpha$, As$L\alpha$ and S$K\alpha$.

Most of the SIMS analyses were done at CANMET (Ottawa), with a limited number performed at the Université de Montpellier II. At Montpellier, some analyses for trace Pt were done using a hybrid Cameca secondary-ion mass spectrometer described as partly an IMS–4f model with features of an IMS–5f model. Operating conditions were similar to those at CANMET (Table 5), except that very low currents of 60 to 70 nA were used. Local calibrations of the magnet were made, followed by depth profiles on implanted standards, as described by Cabri & McMahon (1995). To provide a reference mass for subsequent calculations of the Relative Sensitivity Factor (RSF), as well as to monitor the system's stability and the integrity of the sample, one or two other masses were recorded (*e.g.*, ^{56}Fe, $^{57}Fe_2 + {}^{32}S$, $^{62}Ni_2 + {}^{32}S$). Calibrations and some computations were done using the Cameca SIMS version 5.2 program, and calculations of RSF, peak and curve concentrations were done off-line using Excel. The depth profiles of the implant standards were measured at the Centre d'Electronique de Montpellier.

At CANMET, the analyses for trace Pt and Au were done using a Cameca IMS–4f double-focusing magnetic sector secondary-ion mass spectrometer. Details of the operating conditions are listed in Table 5. The usual practice was to perform two consecutive depth-profiles on an implant standard before the mineral analyses, followed by one or two additional depth-profiles of the same implant standard at the end of the series of mineral analyses. Crater depths in the implant standard were measured using a Tencor Alpha–Step 200 profilometer several times in both directions, and RSF values were calculated using the SIMS Instrument Control System software, version 4.0, from Charles Evans and Associates. For the analyses of pentlandite, the integrated counts for ^{198}Pt and the reference mass(es) were measured from each spectrum and used, together with the average RSF value, to calculate the concentration of platinum in ppm by weight. Trace concentrations in awaruite and heazlewoodite could not be calculated in the same manner because no standards were available. For awaruite, a grain (AW5) found to contain relatively high Pt was later analyzed by electron microprobe (in the above-described analytical conditions). Sixteen point-analyses gave an average of 0.014 wt% Pt (with a standard deviation of 0.009), and the following average composition (in wt%): Fe 19.861 (σ 0.367), As 0.018 (0.029), Co 0.417 (0.015), Ni 78.832 (0.325), Cu 1.684 (0.089). The RSF was calculated using the concentration of 0.014 wt% Pt obtained by EPMA. Thus, the integrated counts for ^{198}Pt and the ^{62}Ni reference mass for each spectrum were used with this RSF to calculate the Pt concentration of each grain. It was not possible to quantify the Pt concentration of heazlewoodite because no grain was found with sufficient Pt to analyze with the electron microprobe. Direct-ion images of selected elemental and molecular ion species were acquired by operating the instrument in the ion microscope mode while retaining high mass-resolution. For the present study, acquisition times of 60 s were used.

Results of the SIMS Analyses

The first SIMS analyses, which were done at Montpellier, showed that awaruite and pentlandite contain Pt, but we did not detect Pt in heazlewoodite. Further depth profiles and ion images done at CANMET confirmed these preliminary observations. These depth profiles were done on eight grains of awaruite, all of which were found to contain Pt, and were followed by ion images. However, difficulties in focusing the images required that the polished section be repolished. A further 14 awaruite grains were then analyzed on the new polished surface, and ion images prepared for selected grains containing both awaruite and heazlewoodite. A grain with relatively high Pt counts was chosen for an EPMA analysis in order to have a reference standard for Pt in awaruite (grain AW5, see above). The results of the SIMS analyses for all awaruite grains are given in Table 6 and show a range from 0.002 to 0.121 wt% Pt.

TABLE 6. RESULTS OF SIMS ANALYSES OF AWARUITE FROM YATÉ 1*

Date	Gr. No.	Pt	Date	Gr. No.	Pt	Date	Gr. No.	Pt
26-Feb	AW-1	0.002	26-Mar	AW5**	0.014			
26-Feb	AW-2	0.018	26-Mar	AW1	0.002	26-Mar	AW9	0.005
26-Feb	AW-3	0.011	26-Mar	AW2	0.024	26-Mar	AW12	0.0004
26-Feb	AW-4	0.121	26-Mar	AW3	0.015	26-Mar	AW13r	0.002
26-Feb	AW-5	0.014	26-Mar	AW4	0.006	26-Mar	AW15	0.006
26-Feb	AW-6	0.010	26-Mar	AW6	0.055	26-Mar	AW16	0.009
26-Feb	AW-7	0.004	26-Mar	AW7	0.009	26-Mar	AW17	0.009
26-Feb	UK-1	0.004	26-Mar	AW8	0.008			

*Sample 165-1, section #53636 (SI-2); **Grain analyzed by electron microprobe in 1997. Note: polished section was repolished for the 26 March analyses, making it impossible to recognize grains previously analyzed. The concentration of Pt is quoted in wt%.

SIMS ion images were performed on a section containing two grains of awaruite, one of which (grain 1) is euhedral, and the other (grain 2) anhedral with a small inclusion of pentlandite (Fig. 6). The analyzed section also contains part of a large crystal of heazlewoodite. The major-element compositions of these grains are given in Tables 2 and 3.

A slight difference in composition is noted between awaruite 1 and 2. Awaruite 1 is slightly enriched in Ni and Co and impoverished in Fe and Cu compared to

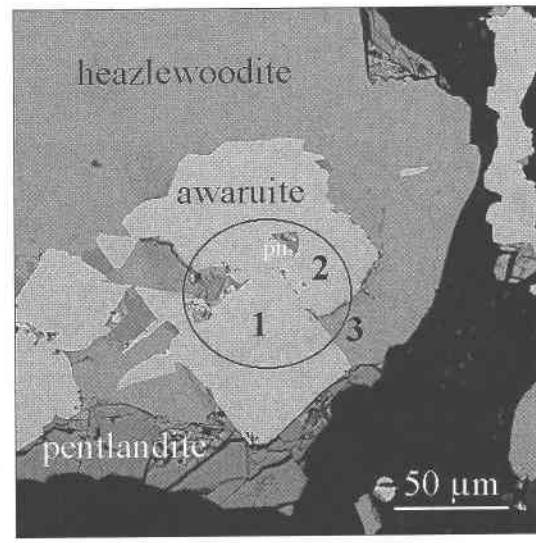

FIG. 6. BSE image showing enlargement of awaruite and heazlewoodite association in sample 165–1 (Yaté 1). The area within the ellipse represents the area shown on SIMS ion images in Figure 7, approximately 62.5 µm in diameter. Areas 1 and 2 represent awaruite, and area 3 represents heazlewoodite; pn: pentlandite inclusions in awaruite area 2.

awaruite 2, but these differences (less than 1% for the major elements) are very minor compared to the large Ni-for-Fe substitution recorded in Figure 5. The SIMS ion images confirm that Pt favors awaruite over heazlewoodite, but clearly show that awaruite 1 is much more enriched in Pt than awaruite 2 (Figs. 6, 7); note that the Pt content has not been quantified. It seems that Pt is preferentially concentrated in awaruite containing less Fe and Cu and more Ni and Co, but this has not been systematically studied. In addition, it can be seen that both awaruite grains also host gold (Fig. 7F), in contrast to heazlewoodite, which hosts none.

Eleven grains of pentlandite were analyzed by SIMS (Table 7). The analyses show that pentlandite contains from about 1 to 10 ppm Pt, considerably less than awaruite. This range is comparable to a range of 1 to 18 ppm Pt recently reported for most pentlandite grains analyzed from the Main Sulfide Zone, Great Dyke, Zimbabwe (Oberthür *et al.* 1997). In contrast to pentlandite and awaruite, 10 of 12 grains of heazlewoodite are without detectable Pt in SIMS depth profiles. For the two heazlewoodite grains with a few Pt counts, it was not possible to quantify their Pt content, but the concentration is estimated to be less than or close to 1 ppm.

The preferential association of Pt in awaruite over heazlewoodite is in contrast to the preliminary findings on samples on unknown origin reported by Lindsay & Sellschop (1988). These authors showed a SIMS linescan through heazlewoodite, bornite–chalcocite, Ni–Cu–Fe alloy and back into heazlewoodite and interpreted the ^{194}Pt concentration as being highest in heazlewoodite and lowest in bornite–chalcocite. They also interpreted Au as being most enriched in bornite–chalcocite. Though we have no Cu sulfides in our samples, we have demonstrated a clear preference of Pt and Au for awaruite over heazlewoodite. A later, more comprehensive publication (Lindsay *et al.* 1994) shows that Pt and other PGE are enriched in Fe–Ni alloy in furnace (Fe–Ni–S) matte and in Cu–Ni alloy in converter (Cu–Ni–S) matte, which is more in agreement with our results. In reference to their earlier exploratory qualitative work, they wrote: "SIMS imaging of converter matte revealed that trace (parts per million) quantities of PGE are homogeneously distributed in sulphides. Heazlewoodite hosts Pt, Pd, Ir and Os, bornite hosts Au and minor Rh, and chalcocite hosts Rh...". A quantitative study of trace PGE in different mattes would help provide more precise data and should also benefit the pyrometallurgical processing of PGE ores.

TABLE 7. RESULTS OF SIMS ANALYSES OF PENTLANDITE FROM YATÉ 1*

Date	Sample	Gr. No.	Pt	Reference mass	Standard	Location
7 Dec '95	SI-1	178	9.9	156	PN-92-12	Montpellier
7 Dec '95	SI-8	185	8.5	156	PN-92-12	Montpellier
23 Feb '96	SI-8	PN-1	5.3	144	PN-92-18	Ottawa
23 Feb '96	SI-8	PN-2	2.4	144	PN-92-18	Ottawa
23 Feb '96	SI-8	PN-3	5.9	144	PN-92-18	Ottawa
23 Feb '96	SI-8	PN-3A**	1.3	144	PN-92-18	Ottawa
26 Mar '96	SI-8	PN-3	<0.3	156	PN-92-18	Ottawa
26 Mar '96	SI-8	PN-5	5.7	156	PN-92-18	Ottawa
26 Mar '96	SI-8	PN-6	1.3	156	PN-92-18	Ottawa
26 Mar '96	SI-8	PN-7	<0.3	156	PN-92-18	Ottawa
26 Mar '96	SI-8	PN-8	<0.3	156	PN-92-18	Ottawa

*Sample 165-1, section #53636 (SI-2); **same grain as #185, but middle of grain. Note: polished section repolished for the 26 March analyses, making it impossible to recognize grains previously analyzed. The concentration of Pt is quoted in ppm.

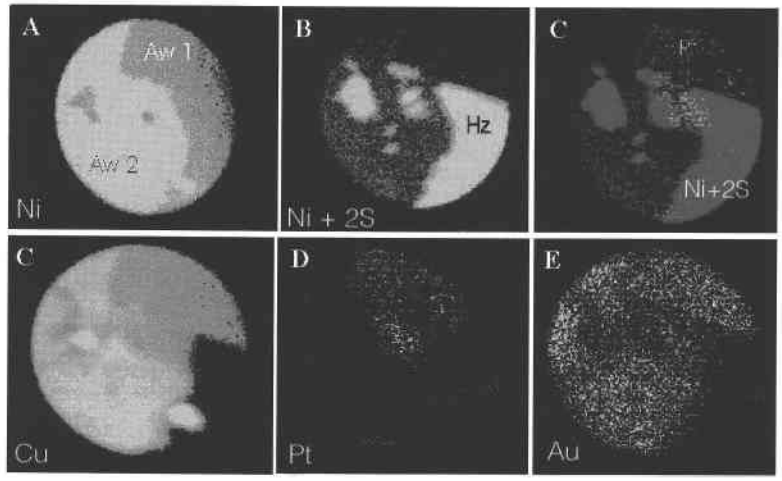

FIG. 7. SIMS ion images, all 62.5 μm in diameter. A. ^{62}Ni. B. ^{62}Ni + ^{32}S + ^{34}S. C. Overlay of ^{62}Ni + ^{32}S + ^{34}S on image of ^{195}Pt. The Pt can be seen to concentrate mainly in the awaruite crystal (area 1) and not in heazlewoodite or the pentlandite inclusions in awaruite of area 2. D. ^{63}Cu. E. ^{195}Pt. F. ^{197}Au.

Discussion and Conclusions

In this study, we have shown that PGE enrichment occurs in sulfides and metallic alloys in mantle harzburgites, and that Pt concentrates preferentially in awaruite as opposed to sulfides. The origin of these sulfide and metallic-alloy minerals is, however, still controversial. Their textures suggest that they appeared very early, at magmatic conditions, but their composition was probably modified later, particularly during serpentinization. The PGE enrichment of the sulfides probably occurred contemporaneously with crystallization of the primary sulfide assemblage, with most of the PGE initially in solid solution in the sulfides. Had primary platinum-group minerals been present, they would probably not have been entirely affected by the transformation processes during the serpentinization that affected the BMS, and remnants of PGM would have been found.

Some authors (*e.g.*, Krishnarao 1964, Sinton 1976) consider that the assemblage described here, consisting of heazlewoodite, pentlandite, and awaruite, is specific to serpentinization. Peretti *et al.* (1992) have shown an assemblage consisting of pentlandite, awaruite, magnetite, native copper and silicates that formed during metamorphism in a peridotite under strongly reducing conditions. Experimental studies (Filippidis 1985) have shown that serpentinization of olivine at very low sulfur fugacity produces an assemblage consisting of heazlewoodite, Ni-poor magnetite and Ni-poor awaruite, whereas the opaque assemblage in the sulfur-free system consists of Ni-rich magnetite and Ni-rich awaruite. Many other authors have described the effect of serpentinization on sulfide assemblages and the possibility of generating Ni–Fe sulfide and alloys from silicates (Eckstrand 1975, Lorand 1989). On the other hand, Lorand *et al.* (1993) suggested that the PGE enrichment for the Lanzo lherzolite massif was due to an ascending magma (S-saturated melt) that percolated through the peridotite (*i.e.*, magmatic conditions).

The hypothesis favored here is that an immiscible magmatic sulfide liquid (i) formed from a percolating ascending magma in the mantle (or from an early fluid under subsolidus conditions as opposed to a serpentinization-related fluid), (ii) became enriched in PGE as a result of a high *R* factor (*i.e.*, a large amount of a S-saturated magma percolating through the residual mantle provoking collection of the PGE by sulfides), and (iii) then crystallized, giving a "magmatic" sulfide assemblage with Ni-sulfides, Fe-sulfides and minor Cu-sulfides. In a second stage, because of reducing conditions presumably imposed during serpentinization (*cf.* presence of graphite), this mineral assemblage would be modified to give the observed mineral association.

The transformation of the magmatic sulfides and the formation of the Ni–Fe alloys resulted in a redistribution of the PGE in the ore minerals. Thus Pt is strongly partitioned in the Ni–Fe alloy (in agreement with its siderophile character). The distribution of the other PGE has not been studied at the trace-element scale in the minerals, although we have noted a strong Pd enrichment in a sample with abundant pentlandite.

The conditions for PGE redistribution in the secondary ore assemblage are totally unknown, but this redistribution remains at the scale of the ore-mineral assemblage. If fluids were involved in the transformation of the primary magmatic assemblage, they must also have been involved in the redistribution of the PGE.

This study has shown for the first time that Pt can be strongly reconcentrated in the alloy, and that the Pt content in awaruite is very varied (from 20 to 1210 ppm). This heterogeneity occurs at the scale of the crystal, as shown in Figures 6 and 7. Grain 1 (euhedral) is much more enriched in Pt than grain 2 (anhedral). We do not believe, at this stage of the study, that the small difference in composition between grains 1 and 2 can account for the distribution of Pt. We believe rather that Pt was concentrated first in the early euhedral crystals then, when the residual Pt content of the fluid was very low, awaruite 2 was formed. The presence of Au in awaruite was also not suspected (and has not been quantified). Both generations of awaruite seem to be equally enriched in Au, whereas the sulfides (heazlewoodite and pentlandite) seem to be totally devoid of Au.

High levels of Pt had already been recorded in samples from the New Caledonia ophiolite, with a typical PGE distribution characterized by a strong Pt anomaly (Augé & Maurizot 1995). These enrichments are associated with chromite-bearing rocks occurring as dykes at the base of the cumulate series; these are typically devoid of sulfides. It was shown that they belong to a late-magmatic stage, but the relationship between this PGE mineralizing event and the PGE enrichment in the mantle cannot be evaluated.

The PGE distribution in the sulfides and metallic alloys is variable and seems to be partly controlled by the mineral assemblage, Pd-rich samples being relatively enriched in pentlandite. This characteristic is probably a remnant of the primary mineralization, with the strong affinity of Pd for pentlandite being well demonstrated. Thus the Pt/Pd value in the ore minerals varies between 0.17 and 2.58, the Pt-rich samples being also enriched in Ir, whereas high Rh values are obtained both in Pd-rich and Pd-poor samples.

The PGE values in the ore minerals obtained in this study are well above some published values for other ophiolites containing sulfide mineralization in the mantle series. For example, Economou & Naldrett (1984) gave an average of 179 ppb Pt, 9 ppb Pd and 16 ppb Rh (values recalculated to 100% sulfides) for samples containing various amounts of pyrrhotite, chalcopyrite, magnetite and chromite. These authors interpreted this mineralization as having precipitated from hydrothermal fluids, the sources of the metals being the rocks themselves.

Enrichments in PGE are also rather common in the series of mafic–ultramafic cumulates in ophiolites.

Lachize *et al.* (1991) described a maximum of 37 ppb Pt, 130 ppb Pd and 4 ppb Rh in the sulfide-rich samples from gabbro cumulates of the Oman ophiolite. The sulfides have a magmatic origin, having precipitated as droplets of immiscible liquid from a mafic magma. Ohnenstetter *et al.* (1991) described Pd enrichment in cumulate dunite enriched in pentlandite (Albanian ophiolite), and Pedersen *et al.* (1993) described Pt–Pd enrichment in a sulfide-bearing horizon from olivine cumulates in the Leka ophiolite complex, Norway. Obviously, PGE enrichment in "residual" mantle rocks cannot be explained in terms of simple magmatic segregation of a cumulate phase.

Amongst the unsolved problems is the origin of the awaruite grains associated with the symplectite, and the conditions of formation of the reaction rim between awaruite and chromite in certain types of symplectite. There is no indication that the awaruite associated with the BMS assemblage was derived by the same process as the awaruite associated with the chromite–silicate symplectite.

In conclusion, we have shown that PGE (other than Os, Ir and Ru, which are classically associated with chromite) can be found in an ophiolitic environment, and that ophiolite sources were not necessarily devoid of Pt, Pd and Rh. Our findings also confirm that SIMS is a suitable tool in the study of trace concentrations of PGE and Au ore in minerals and for obtaining images on the distribution of these elements among different minerals. However, much more work is needed to fully document the trace-element distributions in this and related associations.

Acknowledgements

This article is BRGM contribution number 98041. This work was partly supported by a BRGM research project. Analytical work by LJC at the Université de Montpellier II was partly funded by the Ministère de l'Education nationale, de la Recherche et de la Technologie, Paris, France. The authors are grateful to the following for technical support: at Montpellier, Dr. J.-M. Luck, Mr. J. Kieffer and Mme I. Salesse; at CANMET, Messrs. M. Beaulne, V. Chartrand and J.H.G. Laflamme; at BRGM, MM. C. Gilles and P. Jézéquel. Editor R.F. Martin and the reviewers, E.H. Kinloch and R.P. Schouwstra, are acknowledged for having considerably improved this paper.

References

Ahmed, Z. & Bevan, J.C. (1981): Awaruite, iridian awaruite, and a new Ru–Os–Ir–Ni–Fe alloy from the Sakhakot–Qila complex, Malakand Agency, Pakistan. *Mineral. Mag.* **44**, 225-230.

Aubouin, J., Mattauer, M. & Allègre, C.J. (1977): La couronne ophiolitique périaustralienne: un charriage océanique représentatif des stades précoces de l'évolution alpine. *C.R. Acad. Sci. Paris* **285**, *Sér.* **D**, 953-956.

Augé, T. & Maurizot, P. (1995): Stratiform and alluvial platinum mineralization in the New Caledonia ophiolite complex. *Can. Mineral.* **33**, 1023-1045.

_____, _____, Breton, J., Eberlé, J.M., Gilles, C., Jézéquel, P., Mézière, J. & Robert, M. (1995): Magmatic and supergene platinum-group minerals in the New Caledonia ophiolite. *Chron. Rech. Min.* **63**(520), 3-26.

Cabri, L.J. & McMahon, G. (1995): SIMS analysis of sulfide minerals for Pt and Au: methodology and relative sensitivity factors (RSF). *Can. Mineral.* **33**, 349-359.

Cocherie, A. Volfinger, M. & Meyer, G. (1987): Determination of the noble metals in chromites and other geological materials by radiochemical neutron activation analysis. *J. Radioanal. Nuclear Chem.* **113**, 133-143.

Eckstrand, O.R. (1975): The Dumont serpentinite: a model for control of nickeliferous opaque mineral assemblages by alteration reactions in ultramafic rocks. *Econ. Geol.* **70**,183-201.

Economou, M.I. & Naldrett, A.J. (1984): Sulfides associated with podiform bodies of chromite at Tsangli, Eretria, Greece. *Mineral. Deposita* **19**, 289-297.

Field, S.W. & Haggerty, S.E. (1994): Symplectites in upper mantle peridotites: development and implications for the growth of subsolidus garnet, pyroxene and spinel. *Contrib. Mineral. Petrol.* **118**, 138-156.

Filippidis, A. (1985): Formation of awaruite in the system Ni–Fe–Mg–Si–O–H–S and olivine hydration with NaOH solution, an experimental study. *Econ. Geol.* **80**, 1974-1980.

Glasser, M. (1904): Richesses minérales de la Nouvelle-Calédonie. *Annales des Mines, Sér.* **10**, **5**, 540-541.

Guillon, J.H. (1969): Sur la fréquence des sulfures métalliques dans les massifs péridotitiques de la Nouvelle-Calédonie. *C.R. Acad. Sci. Paris* **268**, *Sér.* **D**, 3013-3014.

_____ & Lawrence, L.J. (1973): The opaque minerals of the ultramafic rocks of New Caledonia, *Mineral. Deposita* **8**, 115-126.

_____ & Saos, J.L. (1971): Les règles de distribution des sulfures cupro-nickelifères dans les massifs ultrabasiques de Nouvelle-Calédonie. *Publication ORSTOM, Centre de Nouméa.*

Johan, Z. & Augé, T. (1986): Ophiolitic mantle sequences and their evolution: mineral chemistry constraints. *In* Metallogeny of Basic and Ultrabasic Rocks (M.J. Gallagher, R.A. Ixer, C.R. Neary & H.M. Prichard, eds.). The Institution of Mining and Metallurgy, London, U.K. (305-317).

Krishnarao, J.S.R. (1964): Native nickel–iron alloy, its mode of occurrence, distribution and origin. *Econ. Geol.* **59**, 443-448.

LACHIZE, M., LORAND, J.P. & JUTEAU, T. (1991): Cu–Ni–PGE magmatic sulfide ores and their host layered gabbros in the Haymiliyah fossil magma chamber (Haylayn block, Semail ophiolite nappe, Oman). *In* Ophiolite Genesis and Evolution of the Oceanic Lithosphere (T. Peters, A. Nicolas & R.G. Coleman, eds.). Kluwer, Dordrecht, The Netherlands (209-229).

LINDSAY, N.M. & SELLSCHOP, J.P.F. (1988): Routine SIMS microanalysis: trace Au and Pt in sulfides. *Nuclear Instrum. Methods Phys. Res.* **B35**, 358-363.

_____, TREDOUX, M. & SELLSCHOP, F. (1994): Mineralogical evaluation of PGE behaviour in Fe–Ni–S and Cu–Ni–S mattes and fayalite slag: geological implications. *Austral. Inst. Mining Metall. Proc.* **299**(2), 95-106.

LORAND, J.P. (1989): Mineralogy and chemistry of Cu–Fe–Ni sulfides in orogenic-type spinel peridotite bodies from Ariege (northeastern Pyrenees, France). *Contrib. Mineral. Petrol.* **103**, 335- 345.

_____, KEAYS, R.R. & BODINIER, J.L. (1993): Copper and noble metal enrichments across the lithosphere–asthenosphere boundary of mantle diapirs: evidence from the Lanzo lherzolite massif. *J. Petrol.* **34**, 1111-1140.

MOUTTE, J. (1982): Chromite deposits of the Tiébaghi ultramafic massif, New Caledonia. *Econ. Geol.* **77**, 576-591.

OBERTHÜR, T., CABRI, L.J., WEISER, T.W., MCMAHON, G. & MÜLLER, P. (1997): Pt, Pd and other trace elements in sulfides of the Main Sulfide Zone, Great Dyke, Zimbabwe: a reconnaissance study. *Can. Mineral.* **35**, 597-609.

OHNENSTETTER, M., KARAJ, N., NEZIRAJ, A., JOHAN, Z. & CINA, A. (1991): Le potentiel platinifère des ophiolites: minéralisations en éléments du groupe du platine (PGE) dans les massifs de Tropoja et Bulqiza, Albanie. *C.R. Acad. Sci. Paris* **313**, *Sér.* **II**, 201-208.

PARIS, J.-P., ANDREIEFF, P. & COUDRAY, J. (1979): Sur l'âge éocène supérieur de la mise en place de la nappe ophiolitique de Nouvelle-Calédonie, unité du charriage océanique périaustralien, déduit d'observations nouvelles sur la série de Népoui. *C.R. Acad. Sci. Paris* **288**, *Sér.* **D**, 1659-1661.

PEDERSEN, R.B., JOHANNSEN, G.M. & BOYD, R. (1993): Stratiform platinum-group element mineralizations in the ultramafic cumulates of the Leka ophiolite complex, central Norway. *Econ. Geol.* **88**, 782-803.

PERETTI, A., DUBESSY, J., MULLIS, J., FROST, B.R. & TROMMSDORFF, V. (1992): Highly reducing conditions during Alpine metamorphism of the Malenco peridotite (Sondrio, northern Italy) indicated by mineral paragenesis and H_2 in fluid inclusions. *Contrib. Mineral. Petrol.* **112**, 329-340.

PICOT, P. (1959): Sur la présence de minerais métalliques nickélifères dans les serpentines. *Bull. Soc. Fr. Minéral. Cristallogr.* **82**, 329-334.

PRINZHOFER, A., NICOLAS, A., CASSARD, D., MOUTTE, J., LEBLANC, M., PARIS, J.P. & RABINOVITCH, M. (1980): Structure in the New Caledonia peridotites–gabbros: implications for oceanic mantle and crust. *Tectonophys.* **69**, 85-122.

RAMDOHR, P. (1967): A widespread mineral association, connected with serpentinization with notes on some new or insufficiently defined minerals. *Neues Jahrb. Mineral., Abh.* **107**, 241-265.

SAOS, J.L. (1972): *Contribution à l'étude de la répartition des sulfures cupronickélifères dans les ultrabasites de Nouvelle-Calédonie*. Thèse, Université des Sciences et Techniques du Languedoc, Montpellier, France.

SINTON, J.J. (1976): Compositional relationships of Fe–Ni alloy and coexisting phases in serpentinite, Red Mountain, New Zealand. *Mineral. Mag.* **40**, 792-794.

VOLFINGER, M. (1989): Determination of rhodium in geomaterials by high-energy alpha-particle activation. *J. Radioanal. Nuclear Chem.* **131**, 19-35.

Received January 11, 1999, revised manuscript accepted August 18, 1999.